Electronic Supplementary Material (ESI) for RSC Advances.

Supporting Information

Electrochromism and electrochemical properties of complexes of transition metal ions with benzimidazole-based ligand

Monika Wałęsa-Chorab,[a*] Radosław Banasz,[a] Damian Marcinkowski,[a,b] Maciej Kubicki,[a] Violetta Patroniak[a]

[a]*Faculty of Chemistry, Adam Mickiewicz University, Umultowska 89b, 61614 Poznań, Poland*
[b] *Current address: Institute of Technology and Life Sciences, Biskupińska 67, 60-463 Poznań, Poland*

**Corresponding author: E-mail: mchorab@amu.edu.pl; Fax: +48 618291508; Tel: +48 618291772*

Table of contents

Figure S1. Spectral changes of 1 in dehydrated and deaerated acetonitrile with 0.1 M $TBAPF_6$ as a supporting electrolyte by applying +1200 (■), +1300 (●), +1400 (▲), +1500 (▼) and +1600 mV (♦) potentials versus Ag/AgCl gel reference electrode held for 30 s per potential. Insert: photographs of the original (left) and electrochemically oxidized (right) 1 by applying a potential for 1 min. 3
Figure S2. Spectral changes of 3 in dehydrated and deaerated acetonitrile with 0.1 M $TBAPF_6$ as a supporting electrolyte by applying 0 (■), -500 (●), -600 (▲) and -700 mV (▼) potentials versus Ag/AgCl gel reference electrode held for 30 s per potential. Insert: photographs of the original (left) and electrochemically reduced (right) 3 by applying a potential for 1 min. 3
Figure S3. Spectral changes of 4 in dehydrated and deaerated acetonitrile with 0.1 M $TBAPF_6$ as a supporting electrolyte by applying 0 (■), -500 (●), -600 (▲), -700 (▼) and -800 mV (♦) potentials versus Ag/AgCl gel reference electrode held for 30 s per potential. Insert: photographs of the original (left) and electrochemically reduced (right) 4 by applying a potential for 1 min. 4
Figure S4. Spectral changes of 5 in dehydrated and deaerated acetonitrile with 0.1 M $TBAPF_6$ as a supporting electrolyte by applying +400 (■), +500 (●), +600 (▲), +700 (▼), +800 (♦), +1000 (►), +1100 (○), +1200 (□) and +1300 mV (Δ) potentials versus Ag/AgCl gel reference electrode held for 30 s per potential. Insert: photographs of the original (left) and electrochemically oxidized (right) 5 by applying a potential for 1 min. 4
Figure S5. The cyclic voltammogram (2nd cycle) of Mn(II) complex 6 measured in anhydrous and deaerated acetonitrile with 0.1 M $TBAPF_6$ as a supporting electrolyte at a scan rate 100 mV/s scanned in the negative direction. 5
Figure S11. Changes in transmittance of Cu(II) complex 2 measured in anhydrous and deaerated acetonitrile with 0.1 M $TBAPF_6$ as a supporting electrolyte and monitored at 420 nm when switching between -400 mV and +200 mV potential at 60 s cycles. 5
Figure S12. Changes in transmittance of Cu(II) complex 3 measured in anhydrous and deaerated acetonitrile with 0.1 M $TBAPF_6$ as a supporting electrolyte and monitored at 400 nm when switching between -700 mV and +300 mV potential at 60 s cycles. 6
Figure S13. Changes in transmittance of Cu(II) complex 4 measured in anhydrous and deaerated acetonitrile with 0.1 M $TBAPF_6$ as a supporting electrolyte and monitored at 400 nm when switching between -800 mV and +200 mV potential at 60 s cycles. 6
Figure S9. Changes in transmittance of Co(II) complex 5 measured in anhydrous and deaerated acetonitrile with 0.1 M $TBAPF_6$ as a supporting electrolyte and monitored at 400 nm when switching between -600 mV and +400 mV potential at 60 s cycles. 7

Table S1. CIE coordinates with D65 illuminat and 2° observer angle for the different states of ligand L and its complexes 1-5 in different states. 8
Table S2. Crystal data, data collection and structure refinement. 9

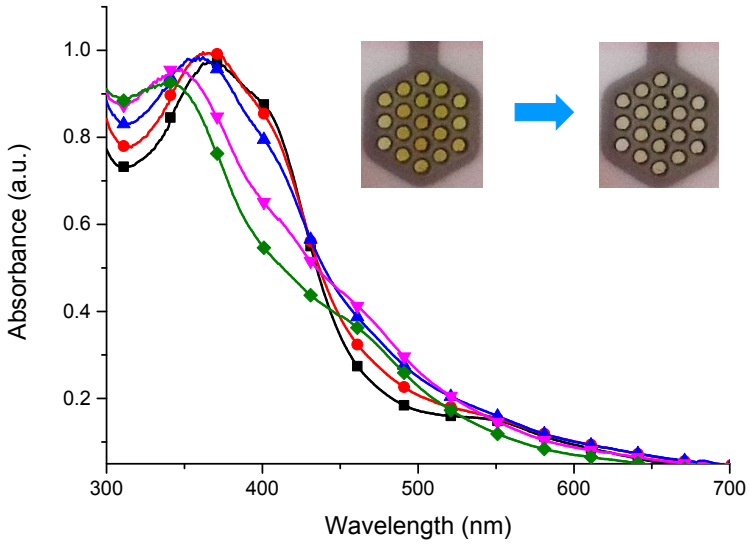

Figure S1. Spectral changes of **1** in dehydrated and deaerated acetonitrile with 0.1 M $TBAPF_6$ as a supporting electrolyte by applying +1200 (■), +1300 (●), +1400 (▲), +1500 (▼) and +1600 mV (♦) potentials versus Ag/AgCl gel reference electrode held for 30 s per potential. Insert: photographs of the original (left) and electrochemically oxidized (right) **1** by applying a potential for 1 min.

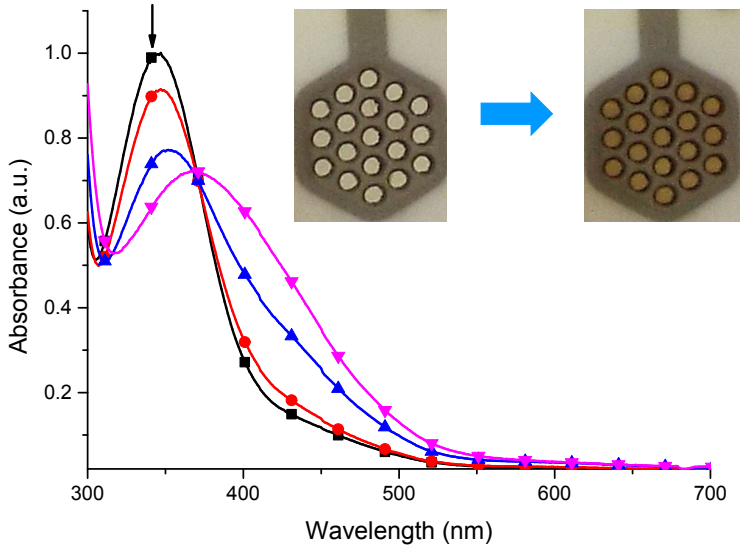

Figure S2. Spectral changes of **3** in dehydrated and deaerated acetonitrile with 0.1 M $TBAPF_6$ as a supporting electrolyte by applying 0 (■), -500 (●), -600 (▲) and -700 mV (▼) potentials versus Ag/AgCl gel reference electrode held for 30 s per potential. Insert: photographs of the original (left) and electrochemically reduced (right) **3** by applying a potential for 1 min.

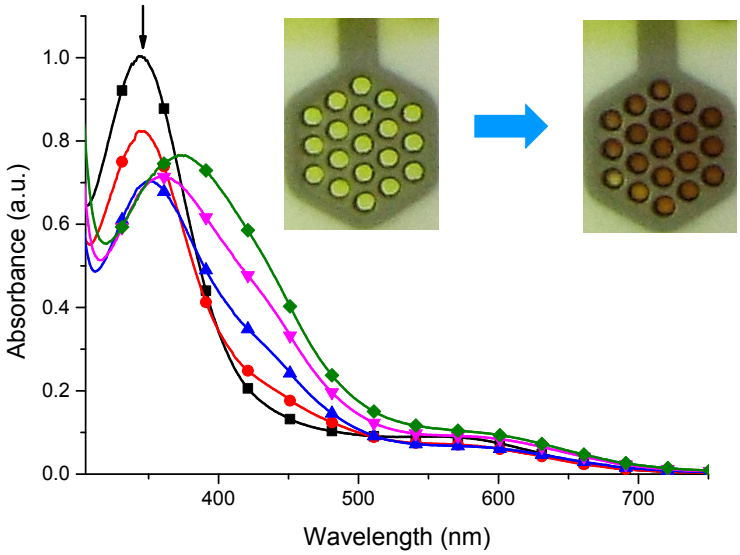

Figure S3. Spectral changes of **4** in dehydrated and deaerated acetonitrile with 0.1 M $TBAPF_6$ as a supporting electrolyte by applying 0 (■), -500 (●), -600 (▲), -700 (▼) and -800 mV (♦) potentials versus Ag/AgCl gel reference electrode held for 30 s per potential. Insert: photographs of the original (left) and electrochemically reduced (right) **4** by applying a potential for 1 min.

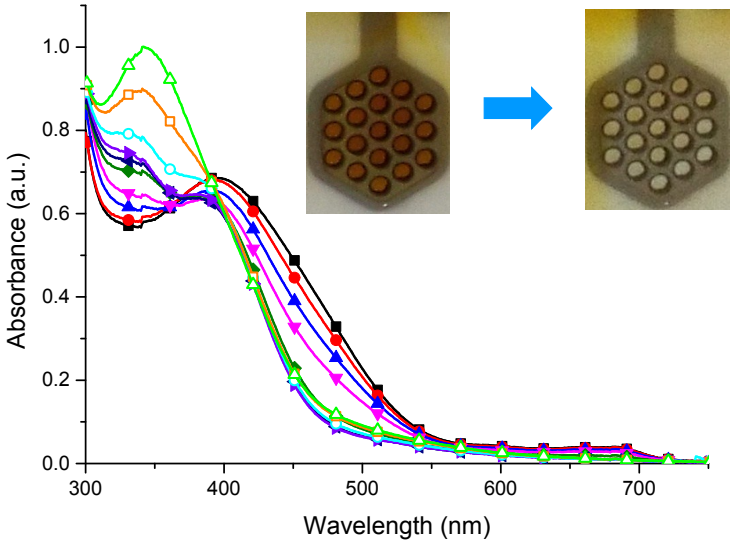

Figure S4. Spectral changes of **5** in dehydrated and deaerated acetonitrile with 0.1 M $TBAPF_6$ as a supporting electrolyte by applying +400 (■), +500 (●), +600 (▲), +700 (▼), +800 (♦), +1000 (▶), +1100 (○), +1200 (□) and +1300 mV (Δ) potentials versus Ag/AgCl gel reference electrode held for 30 s per potential. Insert: photographs of the original (left) and electrochemically oxidized (right) **5** by applying a potential for 1 min.

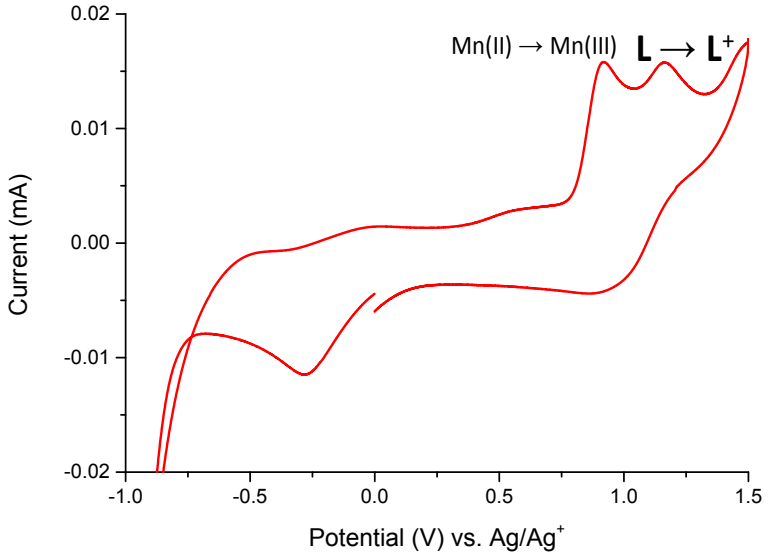

Figure S5. The cyclic voltammogram (2nd cycle) of Mn(II) complex **6** measured in anhydrous and deaerated acetonitrile with 0.1 M $TBAPF_6$ as a supporting electrolyte at a scan rate 100 mV/s scanned in the negative direction.

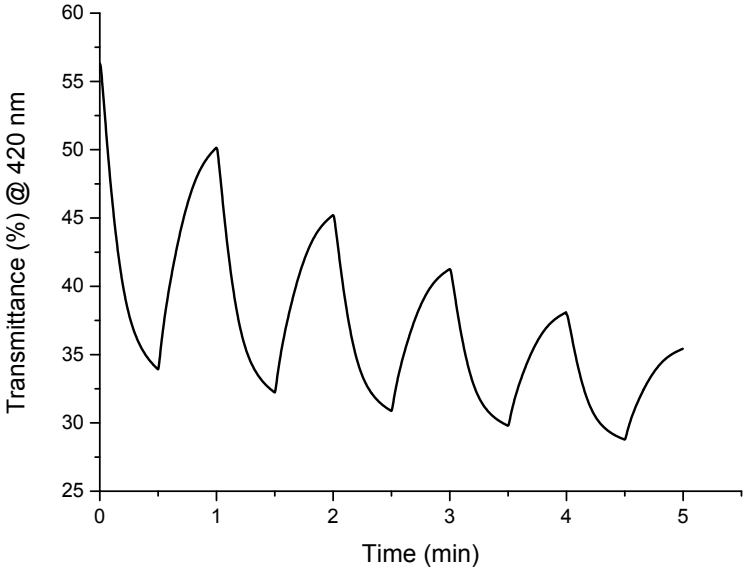

Figure S6. Changes in transmittance of Cu(II) complex **2** measured in anhydrous and deaerated acetonitrile with 0.1 M $TBAPF_6$ as a supporting electrolyte and monitored at 420 nm when switching between -400 mV and +200 mV potential at 60 s cycles.

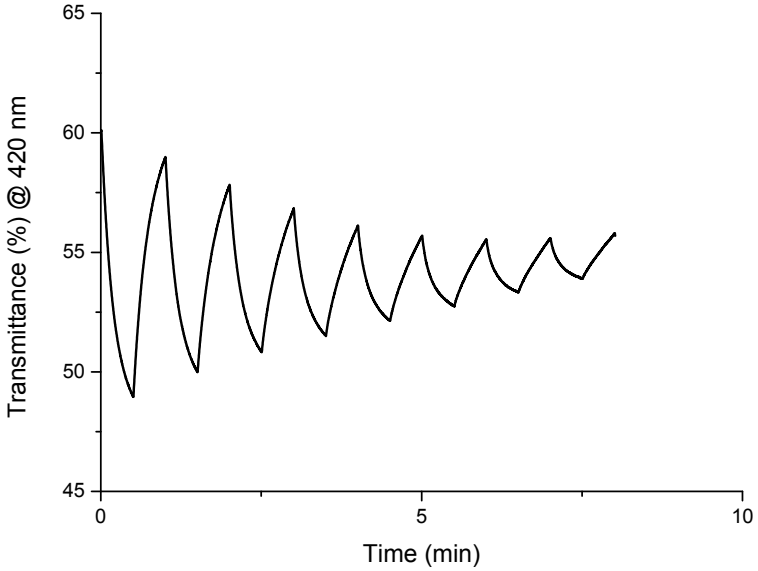

Figure S7. Changes in transmittance of Cu(II) complex **3** measured in anhydrous and deaerated acetonitrile with 0.1 M $TBAPF_6$ as a supporting electrolyte and monitored at 400 nm when switching between -700 mV and +300 mV potential at 60 s cycles.

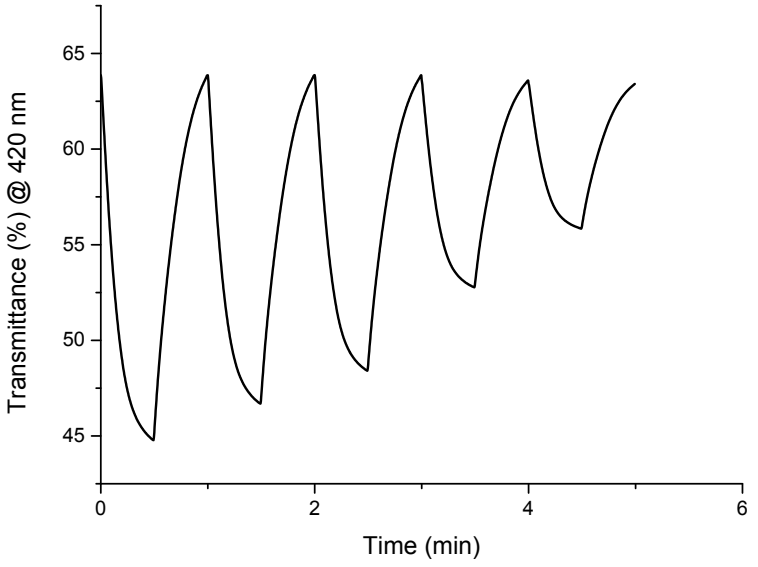

Figure S8. Changes in transmittance of Cu(II) complex **4** measured in anhydrous and deaerated acetonitrile with 0.1 M $TBAPF_6$ as a supporting electrolyte and monitored at 400 nm when switching between -800 mV and +200 mV potential at 60 s cycles.

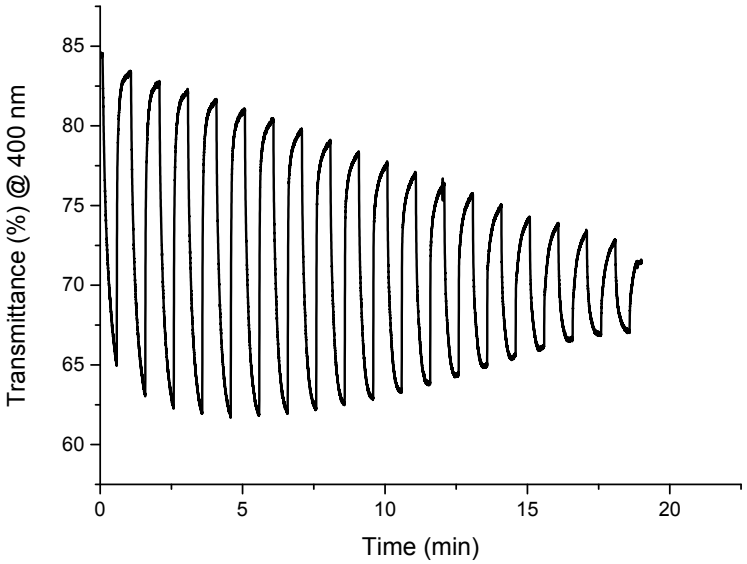

Figure S9. Changes in transmittance of Co(II) complex **5** measured in anhydrous and deaerated acetonitrile with 0.1 M $TBAPF_6$ as a supporting electrolyte and monitored at 400 nm when switching between -600 mV and +400 mV potential at 60 s cycles.

Table S1. CIE coordinates with D65 illuminat and 2° observer angle for the different states of ligand **L** and its complexes **1**-**5** in different states.

Compound		L*	a*	b*
Ligand **L**	Neutral	98.7	-5.5	20.1
	oxidized	98.7	-4.1	12.3
Complex **1**	Neutral	80.3	28.1	-7.5
	1st oxidation state	83.4	2.8	45.3
	2nd oxidation state	82.2	0.2	32.9
	Reduced	79.7	-19.6	33.3
Complex **2**	Neutral	85.6	-6.4	26.15
	Reduced	83.8	10.0	25.4
Complex **3**	Neutral	95.1	-2.7	10.2
	Reduced	93.2	5.8	9.5
Complex **4**	Neutral	80.1	-7.4	30.1
	Reduced	78.8	16.2	27.4
Complex **5**	Neutral	94.6	-5.2	29.9
	1st oxidation state	91.6	15.1	48.5
	2nd oxidation state	95.0	-4.2	16.3

Table S2. Crystal data, data collection and structure refinement.

Compound	**1**	**2**	**3**	**4**	**5**	**6**
Formula	$C_{30}H_{30}FeN_{10}$ $\cdot 2(CF_3O_3S)\cdot CH_3CN$	$C_{18}H_{19}CuF_6N_5O_7S_2$	$C_{16}H_{19}CuN_6O_4^+$ $\cdot NO_3^-$	$C_{15}H_{15}Br_2CuN_5$ $\cdot CH_3OH$	$C_{15}H_{15}Cl_2CoN_5$ $\cdot C_2H_5OH$	$C_{15}H_{15}Br_2MnN_5$
Formula weight	925.68	659.04	484.92	520.72	441.22	480.08
Crystal system	monoclinic	triclinic	monoclinic	triclinic	orthorhombic	triclinic
Space group	$P2_1/n$	P-1	$P2_1/n$	P-1	Pbca	P-1
a(Å)	9.7491(3)	8.0767(3)	9.6735(9)	9.6841(12)	11.59108(13)	7.6305(5)
b(Å)	16.1976(4)	11.3717(5)	17.4644(11)	10.0927(9)	15.95415(19)	8.9863(5)
c(Å)	24.3248(6)	13.9815(8)	12.1452(13)	10.4709(9)	20.3432(3)	13.5352(8)
α(º)	90	76.300(4)	90	91.231(7)	90	83.946(5)
β(º)	95.452(2)	82.265(4)	103.407(10)	92.328(8)	90	75.427(6)
γ(º)	90	85.663(3)	90	117.823(11)	90	67.854(6)
V(Å^3)	3823.80(18)	1234.98(10)	1995.9(3)	903.40(18)	3761.98(8)	831.92(10)
Z	4	2	4	2	8	2
D_x(g cm^{-3})	1.61	1.77	1.61	1.91	1.56	1.92
F(000)	1896	666	996	514	1816	470
μ(mm^{-1})	0.60	1.15	1.15	5.65	9.91	5.60
Reflections:						
collected	14830	8888	7123	5979	18640	5914
unique (R_{int})	7317 (0.019)	5079 (0.015)	3514 (0.021)	3675 (0.017)	3838 (0.057)	3403 (0.019)
with I>2σ(I)	6090	4552	2618	3322	3622	3123
R(F) [I>2σ(I)]	0.050	0.027	0.055	0.028	0.050	0.025
wR(F^2) [I>2σ(I)]	0.122	0.069	0.132	0.071	0.149	0.057
R(F) [all data]	0.061	0.032	0.079	0.033	0.052	0.029
wR(F^2) [all data]	0.130	0.071	0.142	0.074	0.152	0.059
Goodness of fit	1.04	1.04	1.05	1.05	1.05	1.08
max/min Δρ (e Å$^-$	1.50/-0.84	0.39/-0.38	0.80/-0.46	0.8450/-1.02	1.68/-0.61	0.53/-0.49